# A Novel Methodology Using Dexamethasone To Induce Neuronal Differentiation in The CNS-Derived Catecholaminergic CAD Cells

**Ekkaphot Khongkla**
Mahidol University Faculty of Science
**Kwanchanok Uppakara**
Mahidol University Faculty of Science
**Nittaya Boonmuen**
Mahidol University Faculty of Science
**Kanit Bhukhai**
Mahidol University Faculty of Science
**Witchuda Saengsawang** ( witchuda.san@mahidol.ac.th )
Mahidol University Faculty of Science https://orcid.org/0000-0003-0103-6913

**Research Article**

**Keywords:** Cath.a differentiated cell, CAD cells, neuronal cells line, dexamethasone, proliferation, differentiation

**Posted Date:** May 17th, 2021

**DOI:** https://doi.org/10.21203/rs.3.rs-507899/v1

# Abstract

The Cath.a-differentiated (CAD) cell line is a central nervous system-derived catecholaminergic cell line originating from tyrosine hydroxylase (TH)-producing neurons located around the locus coeruleus area of the mouse brain. CAD cells have been used as an *in vitro* model for cellular and molecular studies due to their ability to differentiate under serum-free media conditions. However, the lack of serum-derived survival factors, limits the longevity for differentiated CAD cells to be maintained in healthy conditions; thereby, limiting their use in long-term culture studies. Here, we present a novel differentiation method that utilizes dexamethasone (Dex), a synthetic glucocorticoid receptor agonist. Specifically, we discovered that the addition of 100 μM of Dex into the 1% fetal bovine serum (FBS)-supplemented media effectively induced neuronal differentiation of CAD cells, as characterized by neurite formation and elongation. Dex-differentiated CAD cells exited the cell cycle, stopped proliferating, extended the neurites, and expressed neuronal markers. These effects were dependent on the glucocorticoid receptors (GR) as they were abolished by GR knockdown. Importantly, Dex-differentiated CAD cells showed longer survival duration than serum-free differentiated CAD cells. In addition, RNA-sequencing and qPCR data demonstrate that several genes involved in proliferation, neuronal differentiation, and survival pathways were differentially expressed in the Dex-differentiated cells. This is the first study to reveal Dex as a novel differentiation methodology used to generate postmitotic neuronal CAD cells, which may be utilized as an *in vitro* neuronal model for cellular and molecular neurobiology research.


# Introduction

Cath.a-differentiated (CAD) cells are a neuronal cell line originally established from mouse central nervous system (CNS)-derived catecholaminergic neurons located around the locus coeruleus area of mouse brain (Suri et al. 1993; Qi et al. 1997). CAD cells have been used as an *in vitro* model for studying catecholaminergic neurons, largely because of their ability to be quickly switched from a proliferative phase to a CNS neuron-like differentiation phase by simply removing serum. In serum-supplemented media, cells are undifferentiated and actively proliferate. After serum withdrawal, CAD cells stop proliferating and differentiate into neuron-like cells. Differentiated CAD cells demonstrated a catecholaminergic phenotype, in which they show similar morphologies to primary CNS neurons and express several catecholaminergic neuronal markers (Qi et al. 1997; Pasuit et al. 2004; Muresan and Muresan 2006; Paris et al. 2006; Arboleda et al. 2007; Chesta et al. 2014). Although CAD cells that are differentiated by serum withdrawal exit the cell cycle and morphologically differentiate into neuron-like cells; these cells cannot be effectively maintained for long durations, thereby limiting their applications as *in vitro* neuronal models. Therefore, alternative conditions that effectively differentiate, as well as prolong survival of, CAD cells are necessary.

Glucocorticoids are primary stress-response hormone that are not only synthesized by the adrenal glands but also produced locally by neural progenitor cells (NPCs) (Baulieu 1998; Nürnberg et al. 2018). Glucocorticoid receptors (GR) are broadly expressed in both embryonic and adult NPCs (Sundberg 2006; Fitzsimons et al. 2013; Schouten et al. 2019). The specific GR agonist dexamethasone (Dex) is reported

to dynamically reduce NPC proliferation rates (Sundberg 2006; Bose et al. 2010) and strongly induce neurite outgrowth during differentiation of mouse cortical NPCs (Androutsellis-Theotokis et al. 2013). In addition, Dex has been included in media designed for the differentiation of mesenchymal stem cells into several non-neuronal linages, including adipocytes, osteocytes, and chondrocytes (Derfoul et al. 2006; Ghali et al. 2015). However, the differentiation effect of Dex in neuronal cell lines has never been determined.

Here, we examined the ability of dexamethasone to promote CAD cell differentiation. We investigated the effects of Dex on CAD cell morphology, proliferation, and cell cycle in comparison to serum removal media conditions, which, as stated above, is a conventional differentiation methodology. Survival rates of Dex-differentiated CAD cells were also determined compared to those in serum-free differentiated CAD cells. We additionally performed RNA-sequencing, gene set enrichment analysis, and qPCR to investigate the effect of Dex on differential gene expression. We sought to identify genes that were up- or down-regulated, especially those associated with cell cycle, DNA replication, DNA damage repairs, and cell survival, as well as genes involved in neuronal differentiation and functions. In addition to being the first study to show the effectiveness of Dex as a novel differentiation methodology for a neuronal cell line, this study also reveals the effects of Dex-mediated neuronal differentiation, both at the cellular and molecular level.

# Materials And Methods

### *Cell culture*

CAD cells (ECACC, RRID:CVCL_0199) were cultured as recommended in Dulbecco's Modified Eagle Medium: Nutrient Mixture F-12; DMEM/F12 (catalog number 12500062, Gibco, USA) supplemented with 8% fetal bovine serum (FBS) (catalog number 10270106, HyClone, USA,); 1% antibiotic-antimycotic 100X (catalog number 2185242, Gibco, USA). The cells were maintained in a humidified incubator at 37 °C with 5% $CO_2$ and 95% air (v/v). The passages of cells directed for this study were less than 10. For serum-free induced differentiation, the medium was replaced with DMEM/F12 without serum. For experiments involving Dex-mediated differentiation, the cells were incubated with different concentrations (10, 100 μM) of Dex (catalog number D4902, Sigma-Aldrich, USA) dissolved in DMEM/F12 supplemented with 1% FBS. The cultured media were replenished every 48 h.

### *Cell viability assay*

Cell viability was measured using an MTT assay (catalog number M5655, Sigma-Aldrich, USA). Briefly, the cells were plated on 96-well plates and cultured with different conditions as indicated. The media were removed from each well at the end of the incubation time and replaced with a final concentration of MTT (3-(4,5-dimethyl-thiazol-2-yl)-2,5-diphenyl-tetrazolium bromide, 0.5 mg/ml). The plates were then placed in a humidified incubator at 37 °C with 5% $CO_2$ for an additional 4 h. The insoluble formazan was subsequently dissolved with dimethylsulfoxide; DMSO (catalog number D8418, Sigma-Aldrich, USA). The

colorimetric determination was measured at 570 nm using a Multiskan FC microplate photometer (Thermo Fisher Scientific, USA). Data were normalized as an increased fold change of cell viability from day 0.

### *Knockdown of GR in CAD cells*

GR siRNA (SC-35506) and non-targeting siRNA (SC-37007) were purchased from Santa Cruz Biotechnology (Dellas, Texas, USA). CAD cells were transfected with 40 picomole of GR siRNA or non-targeting siRNA using Lipofectamine 3000 transfection reagent (catalog number L3000008, Thermo Fisher Scientific, USA) according to the manufacturer intructions. The siRNA was diluted in Opti-MEM reduced serum medium (catalog number 31985070, Gibco, USA), mixed with Lipofectamine 3000 reagent and incubated at RT for 15 min. The siRNA- Lipofectamine mixture was then added to the cells. The cells in control group were exposed to the same transfection reagent without the addition of siRNA. Two days after transfection, cells were harvested for Western blot analysis to confirm knockdown efficiency. The knocked-down CAD cells were trypsinized and replated in differentiation medium (100 µM Dex + 1%FBS) for 24 - 72 h. The cells were then assayed via BrdU labeling or immunocytochemistry and imaging for proliferation and differentiation, respectively.

### *Immunocytochemistry and imaging*

In brief, CAD cells were fixed with 4% paraformaldehyde for 20 min and washed three times with 1X phosphate buffer saline (PBS) before being permeabilized with 0.1% Triton X-100 for 10 min. The permeabilized cells were then incubated in 10% BSA (catalog number A2153, Sigma-Aldrich, USA) dissolved in 1X PBS solution to block nonspecific protein binding. After blocking, cells were incubated with mouse monoclonal anti beta-tubulin lll (neuronal), clone 2G10 (RRID:AB_1841228, Sigma-Aldrich, USA) or Rabbit polyclonal anti-Ki-67 antibody (RRID:AB 1841228, Abcam, UK) in 1% BSA/PBS for 1 h at room temperature. Next, cells were incubated with Goat anti-mouse IgG (H+L), superclonal$^{TM}$ recombinant secondary antibody conjugated to Alexa Fluor 488 (caRRID:AB 2536161, Invitrogen, USA) or Goat anti-rabbit IgG (H+L), cross-adsorbed secondary antibody conjugated to Alexa Fluor 594 (RRID:AB 2534095, Thermo Fisher Scientific, USA ) for 1 h at room temperature. DAPI (catalog number D1306, Invitrogen, USA) was used to stain cellular nuclei. The images from each condition were collected from at least 5 non-overlaping areas using a FluoView FV10i laser scanning microscope (Olympus, Japan). To visualize cell morphology, cells from each group were randomly imaged from at least 10 non-overlapping areas using a 10X objective lens on an inverted microscopy ECLIPSE TS100 (Nikon, Japan). All analyses were performed using the Image J version 2.1.0.1.53c software (RRID:SCR_003070, Research Services Branch, National Institute of Mental Health, USA). The cell counter plug-in was used to measure neurite bearing cells. The cells with processes 2-fold longer than the cell body were considered to be neurite containing cells. Neurite length was automately measured using the NeuronJ plug-in, and only traceable neurites with clear neuronal tips were included for the analysis. The length the longest neurite of each cell was traced from the cell body to the end of a process.

### *BrdU assay*

The cell proliferation rate was evaluated using a cell proliferation ELISA, BrdU (colorimetric) assay (reference number 1164722900, lot number 29134900, Roche, Germany). Breifly, CAD cells were plated on a 96-well plates with different conditions and incubated with 10 µM BrdU labelling solution at 37 ºC for 2 h. BrdU-labelled cells were then fixed using the FixDenat solution for 30 min at room temperature. After removing the FixDenat solution, antibody conjugated with peroxidase (anti-BrdU-POD working solution) was added and incubated for 90 min at room temperature. Cells were then washed three times with washing buffer solution (1X PBS) before adding a substrate. The absorbance of the samples was read at 370 and 492 nm using by a Multiskan FC microplate photometer. The subtracted absorbances (370-492 nm) at 24 and 48 h were then normalized to that of 0 h, or relative to control as indicated.

### *Flow cytometry*

To determine the percentage of the cell population in each cell cycle phase, we performed flow cytometry with detection of propidium iodide (PI). CAD cells were plated in T75 flasks and incubated with different conditions and time as indicated. Next, cells were harvested and washed twice with cold 1X PBS and fixed in 70% ethanol at -20°C overnight. On the day of measurement, the pellets were collected by centrifugation and resuspended in 500 µL of PI/RNase A staining buffer (catalog number F10797, Invitrogen, USA). Cells were subsequently incubated in the dark for 15 minutes at room temperature. We then quantified the percentage of cells in each gate of cell cycle, based on the DNA content inside the cells, via the BD FACSCanto II flow cytometer (Amersham Biosciences, USA).

### *Western blot analysis*

Protein lysates from each condition were collected as previously described. In short, CAD cells were washed with cold 1X PBS before being lysed with lysis buffer containing proteases inhibitors cocktail (Complete$^{TM}$ mini, reference number 04693159001, lot number 23160900, Roche, Germany) and phosphatases inhibitors cocktail (phosSTOP$^{TM}$, reference number 04906845001, lot number 45842900, Roche, Germany). Protein concentrations were measured using a Pierce$^{TM}$ bicinchonic acid kit (reference number 23225, lot number UF289331, Thermo Fisher Scientific, USA). An equal amount of protein for each condition was separated by 10% sodium dodecyl sulfate polyacrylamide gel electrophoresis (SDS-PAGE) and then transferred to a polyvinylidene difluoride membrane (catalog number IPVH00010, Millipore, Germany). Non-specific protein binding was blocked with 10% non-fat dry milk in 1X TBST (tris buffer saline with tween 20). The membranes were incubated overnight at 4 °C with Rabbit polyclonal anti-growth associated protein (GAP)-43 (RRID:AB 2107282, Millipore, Germany), Mouse monoclonal anti-GR, clone G5 (catalog number SC-393232, RRID:AB2687823 Santa Cruz Biotechnology, USA), or or Mouse monoclonal anti- GAPDH, clone 6C5 (RRID:AB 2107448, Abcam, USA). Then, membranes were washed and treated with secondary antibody anti-mouse (RRID:AB 2338512) or anti-rabbit (RRID:AB 2307391, Jackson ImmunoResearch, USA), which were conjugated with horseradish peroxidase, diluted in 5% non-fate dry milk in 1X TBST for 1 h at room temperature. Lastly, the protein signal was developed using

enhanced chemiluminescent substrate (catalog number WBLUR500, Millipore, Germany) and detected with hyperfilm (product code 28906839, GE Healthcare, UK). The level of proteins of interest was measured by Image J software (RRID:SCR_003070) and normalized with GAPDH.

### *Double staining apoptosis assay (PI/Hoechst)*

To assess the number of dead cells, CAD cells were double stained with PI (catalog number D1306, Molecular Probes, USA) and Hoechst 33342 (catalog number P1304MP, Sigma-Aldrich, USA), which exhibited a red and blue fluorescence, respectively. PI is used to count dead cells because it is unable to penetrate viable cells, but can label dead cells. Hoechst was used in order to count the total numbers of cells. The fluorescence signals were detected using an Operetta automated widefield microscope (PerkinElmer, USA). Five non-overlapping fields from each well were randomly selected for imaging. Using the Image J software (RRID:SCR_003070), the percentage of dead cells was calculated as the fraction of PI-positive cells relative to the total cell count.

### *Identification of differentially expressed genes (DEG)*

The steps of RNA-seq and its analysis are diagramed in **Supplementary Fig.4A.** Total RNAs were extracted from undifferentiated CAD cells (Pro 1-3) and Dex-differentiated cells (5 days, Dex 1-3) using the TRIzol reagent (reference number 15596026, lot number 262308, Ambion, Life technologies Corporation, USA), according to the manufacturer's instructions. Three independent samples were collected from both experimental groups. RNA concentration and purification were preliminary examined using a Nanodrop$^{TM}$ 2000 spectrophotometer (Thermo Fisher Scientific, USA). Samples then underwent RNA-sequencing analysis at the Omics Sciences and Bioinformatics Center, Chulalongkorn University, Thailand. Quality of the submitted total RNAs were re-evaluated using a Bioanalyzer (Agilent, USA). All mRNA libraries were constructed using 500 ng of input total RNA, as outlined by the QIAseq Standard mRNA Select kit (Qiagen, USA). Briefly, poly-A containing mRNA molecules were initially isolated using magnetic oligo (dT) beads, followed by purification and then fragmentation and cDNA synthesis. QIAseq Beads were used to separate the cDNA from the reaction mix. Subsequently, indexing adapters were ligated to the cDNA, and the cDNA libraries were enriched using 12 cycles, as recommended by the Qiagen CleanStart library amplification protocol. Library quality assurance was conducted using a Bioanalyzer and fluorometer (DeNovix, USA). Next, a library size as recommended by Illumina for this type of library was observed to demonstrate a successful library preparation. Finally, all libraries were combined equally at 10 nM and further diluted to 1.8 pM. The sequencing step was performed on NextSeq with a 75 base-pair end read length. Quality filtered reads were mapped to the mouse reference genome (GRCm38.p6) using the HISAT2 transcript aligner software. Feature Counts software was implemented to obtain raw counts for all mouse genes. The gene counts were used for differential expression analysis with the DESeq2 package to identify differentially expressed genes (DEGs) in the Dex-differentiated CAD cells, as compared to the undifferentiated CAD cells. To judge the significance of DEGs, we used a false discovery rate (FDR) < 0.01 and $\log_2$ [fold change] > 2 or < -2 as the threshold for

delineating upregulated and downregulated expressed genes, respectively. The GEO accession numbers for this database is GSE162087.

### *Gene Set Enrichment Analysis*

The lists of downregulated and upregulated genes were separately subjected to the Database for Annotation, Visualization and Integrated Discovery (DAVID) pathway enrichment analysis (https://david.ncifcrf.gov/ version 6.8.). The enrichment pathways of the Kyoto Encyclopedia of Genes and Genomes (KEGG) and terms of Gene ontology (GO) were judged as the significance at $P<0.05$.

### *Experimental validation with quantitative real-time-PCR*

The mRNA expression of validated genes was determined by real-time quantitative PCR. Briefly, undifferentiated and the Dex-differentiated CAD cells were cultured for 5 days before RNA extraction. RNA concentration and purity were evaluated using a Nanodrop™ 2000 spectrophotometer (Thermo Fisher Scientific, USA). The cDNA was synthesized using iScript™ cDNA synthesis (catalog number 1708841, Bio-Rad, USA) according to the manufacturer's protocol. Quantitative real-time PCR of the validated genes was performed on an equal amount of cDNA from each condition using iTag Universal SYBER® Green supermix (catalog number 1725121, Bio-Rad, USA) with the ABIPRISM-7500 sequence detection system and analysis software (Applied Biosystems, USA). The experiments were repeated in triplicate. The mRNA level of GAPDH was used as an internal control. Ct values of the sample were calculated, and transcript levels were analyzed by the $2^{-\Delta\Delta Ct}$ method. Primers used in this study are listed in **Supplementary Table 1.**

### *Statistical analysis*

Statistical significance was evaluated with GraphPad Prism software, version 8.0 (RRID:SCR 002798, USA) using a Student's t-test or one-way or two way ANOVA, followed by Tukey's multiple comparison test. *P*-values less than 0.05 were considered statistically significant.

## Results

### *Dexamethasone induced differentiation of CAD cells*

While Dex has been reported to induce differentiation of mesenchymal stem cells, no studies have examined its ability to differentiate a neuronal cell line. To test the ability of Dex to induce the differentiation of a neuronal cell line, we examined Dex-induced differentiation of CAD cells. CAD cells were cultured under different conditions, including undifferentiated/proliferative (8% FBS), differentiated (serum-free media), and in the presence of different concentrations of Dex. A low amount of serum (1% FBS) was supplemented to all conditions that were treated with Dex to provide enough growth factors. After 3 days of incubation, the cells in each condition were imaged. Undifferentiated cells were polygonal in shape and were devoid of neurites (**Fig.1A**). Serum-free condition not only caused extended long

neurite processes but also decreased cell number (**Fig.1B, F**). These results are consistent with previous studies (Qi et al. 1997; Bilodeau et al. 2005). Low serum (1%FBS) provided similar effects on CAD cell morphology as the undifferentiation condition. Although cell number was reduced as compared to the undifferentiation condition, it was still much higher than that observed in the differentiation condition (**Fig. 1C, F**). Adding 10 μM Dex to this low-serum condition had no effect on morphology and cell number (**Fig.1D, F**). However, in the presence of 100 μM Dex, the majority of CAD cells extended long neurite processes, similar to those observed in the serum-free differentiated CAD cells (**Fig.1E**). In this condition, cell number was also decreased to almost 4 times less than that of the undifferentiated cells (**Fig.1F**). Importantly, Dex-mediated effects on differentiation and cell number were directly due to Dex treatment, and not the result of exposure to 1% FBS since in the 1% FBS-supplemented condition without Dex, cells remained incompletely differentiated.

Indeed, the induction of differentiation in response to Dex was quite strong since the formation of short processes were observed in some CAD cells even in the presence of 8% serum; however, the neurites were much shorter than the neurites in the Dex + 1% FBS cultures (**Supplementary Fig. 1**). Taken together, these results demonstrate the ability of 100 μM Dex to successfully induce the morphological differentiation in CAD cells like the serum-free condition.

### *Dexamethasone promoted neurite-like formation and elongation in CAD cells*

We further observed the effects of Dex on CAD cell neurite formation and elongation in comparison with the serum-free condition. In the presence of Dex, cells progressively formed more and longer neurites over time, as shown by the percentage of neurite-bearing cells (**Fig.2A and 2B**) and the length of neurites (**Fig.2A and 2C**), respectively. This result was comparable with the serum-free condition.

The effect of Dex-induced neurite formation was quite rapid, as we clearly observed the formation of short neurites protruding from the cell body within 24 hours of Dex (100 μM) treatment (**Fig. 2A**). The number of neurite-presenting cells also significantly increased by 24 h. Most cells extended neurites within three days (**Fig.2B**). The length of neurites in both conditions was continuously increased to nearly 600 μm over the 5 days of differentiation (**Fig.2C**).

To determine whether the differentiated CAD cells express neuronal markers, we labeled for beta-3 tubulin, a neuron-specific protein. We found that beta-3 tubulin was expressed in both undifferentiated and differentiated cells. Nevertheless, the differentiated cells showed stronger fluorescence signals compared to the undifferentiated cells, especially in the neurites, in both SF and Dex differentiation conditions (**Fig. 2D**). The percentage of beta-3 tubulin positive cells was also significantly increased in cells differentiated by both methods relative to undifferentiated cells (**Fig. 2E**). In addition, both SF and Dex differentiation conditions increased the expression of GAP-43, another neuronal marker associated with neurite outgrowth, in differentiated cells relative to the undifferentiated cells (**Fig.2F-G**). These experiments suggest that Dex can effectively promote neurite formation and elongation and that Dex-differentiated CAD cells express neuronal markers similar to serum-free differentiated CAD cells.

### *Dexamethasone induced cell cycle exit and ceased proliferation of the CAD cells*

NPC proliferation is known to be inhibited prior to the neuronal differentiation (Galderisi et al. 2003; Götz and Huttner 2005; Hardwick et al. 2015). As such, we found that Dex treatment resulted in lower CAD cell number than that observed in the undifferentiated group after three days (**Fig.1F**). Therefore, Dex may exert anti-proliferative effects as a mechanism to induce neurite formation. To prove this hypothesis, we assessed the cell proliferation rate using BrdU incorporation assay (**Fig.3A-B**). Cell proliferation was almost completely abolished in the presence of Dex, as evidenced by a significant decrease in BrdU incorporation at 24 h (**Fig.3A**). The anti-proliferative effect of Dex was more rapid than the anti-proliferative effect of the serum-free condition. Specifically, the serum-free condition did not show a significant anti-proliferative effect until 48 h (**Fig. 3B**).

To further evaluate the effect of Dex on cell cycle of CAD cells, we also performed flow cytometry. Consistent with a decrease in cell proliferation rate, the percentage of CAD cells in S phase (i.e., DNA replication phase) was significantly reduced at both 24 and 48h after Dex treatment (**Fig.3C-D**). In contrast, the percentage of the cells entering the G0/G1 phases was significantly increased in both differentiation groups, suggesting that SF and Dex-differentiated cells entered the G0/ G1 phases (**Fig. 3C-D**).

Neurons are postmitotic cells that permanently exit the cell cycle and enter the G0 phase for terminal differentiation. To determine whether the Dex-differentiated CAD cells demonstrated these same properties, we immunolabeled for Ki67, a nuclear protein presenting in all active phases of the cell cycle except in G0 (Kee et al. 2002). We found that Ki67 was clearly expressed in the nucleus of most undifferentiated cells, indicating that these cells were in the proliferating phase. In contrast, Ki67 was absent in the cells treated with serum-free and Dex (**Fig. 3E, F**). These data confirmed that Dex causes CAD cells to cease proliferating and become post-mitotic cells arrested at G0 phase of the cell cycle, thereby resembling neurons.

### *The effects of dexamethasone on CAD cells were mediated by glucocorticoid receptor*

To confirm GR expression and response to Dex in CAD cells, we performed western blot analysis and immunolabeled GR before and after Dex treatment. GR was highly expressed in undifferentiated CAD cells. In the presence of Dex, level of GR in the cytosol was decreased (**Supplementary Fig. 2A-B**), consistent with its increased translocation into the nucleus (**Supplementary Fig. 2C**) indicating that in CAD cells, GR is expressed and can be activated by Dex. In addition, to test whether GR mediated the anti-proliferative and differentiation effects of Dex, GR levels in CAD cells were reduced using siRNA. The siRNA decreased GR protein levels in CAD cells by ~80% (**Fig. 4A-B**). We then investigated the anti-proliferative effect of Dex in GR knocked-down CAD cells using a BrdU incorporation assay. The GR knocked-down CAD cells were differentiated in 100 μM Dex in 1% FBS. As shown in **Fig. 4C,** the proliferative rate indicated by BrdU incorporation was significantly increased by approximately two-fold after 48 h of Dex-mediated differentiation induction in GR knocked-down cells relative to control cells. These results indicate that GR is required for anti-proliferative effect of Dex in CAD cells. We next

determined whether depletion of GR affected the Dex-induced differentiation. After three days of differentiation, we observed that only 50 % of the GR knocked-down CAD cells were neurite positive compared to the control cells **(Fig. 4D, E).** Neurite lengths in the GR knocked-down CAD cells were also shorter than those in the control cells (**Fig. 4D, F)**. These data demonstrate that Dex ceases proliferation and promotes differentiation of CAD cells through GR.

***Dexamethasone prolonged survival of the differentiated CAD cells.***

Above, we demonstrated that 100 μM Dex in 1% FBS effectively inhibits proliferation and induces differentiation, neurite formation, and elongation in the CAD cells. These effects were similar to those of serum-free differentiation media previously published (Qi et al. 1997). However, we found that SF-differentiated cells can be maintained in a healthy stage for only 5 days (**Fig. 5**). Interestingly, in the presence of 100 μM Dex in 1% FBS, differentiated CAD cells can be maintained in healthy condition for at least a month without the need for additional supplements. At day 5 of differentiation, Dex-differentiated cells displayed long, dense neurites, while in the serum-free condition, neurite degeneration can be clearly observed (**Fig. 5A**). In addition, after 5 days of differentiation, double fluorescent staining of PI and Hoechst showed very few dead cells (PI-positive cells) in Dex-differentiated condition, as compared to the serum-free condition, in which 50% of the cells were death (**Fig.5B-C**). The number of surviving cells under each differentiation media was measured up until 30 days. Consistent with previous data, survival of the serum-free differentiated cells gradually declined over the time. Interestingly, throughout these periods, the number of cells that survived in the Dex-differentiated condition remained consistent and was significantly higher than the number of living cells in the serum-free condition (**Fig. 5D**). This increased survival was not observed when CAD cells were treated with 100 μM Dex in serum-free condition (**Supplementary Fig. 3).** Taken together, besides being able to generate neuron-like cells, 100 μM Dex in the 1% FBS-supplemented media also minimizes cell death, suggesting that Dex is an effective differentiation method for generating neuron-like cells from CAD cells.

***Dexamethasone altered the expression of genes involved with proliferation, differentiation and survival in differentiated CAD cells.***

Although the Dex-mediated differentiation has been reported in other cell types (Derfoul et al. 2006; Ghali et al. 2015), the underlying mechanisms remain unclear. Since this is the first study to demonstrate Dex-induced CAD cell differentiation, we wanted to further explore altered gene regulation in such differentiation condition. We performed RNA-sequencing (RNA-seq) analysis to identify genes that are differentially expressed in undifferentiated cells compared to Dex-differentiated cells (**Supplementary Fig. 4A**). Dex-differentiated CAD cells were cultured for 5 days prior to total RNA extraction and analyzed with Illumina-based RNA-seq analysis. The sequence reads (expression level) per sample was obtained in a range of 9.8-11.2 million as shown in **Supplementary table 2**. The high quality of sequence reads was mapped to the mouse reference transcriptome (GRCm38.p6). The gene counts were used for differential expression analysis. Interestingly, many genes were altered in the Dex-differentiated cells. Represented by a volcano plot (**Supplementary Fig. 4B**), a total of 1,183 differentially expressed genes (DEGs) were

identified in the Dex-differentiated CAD cells compared to the undifferentiated CAD cells (false discovery rate < 0.01 and $|\log_2$ [fold change] | > 2). Of these, 803 and 380 genes were significantly upregulated and downregulated in the Dex-differentiated group, respectively. The full list (**Supplementary Excel 1**) and statistical profiling (**Supplementary Fig.5A-C**) of significant DEGs are provided.

To determine the possible biological pathways and functions in which the DEGs are involved, a gene set enrichment analysis was performed using the DAVID database that provides the KEGG pathway and GO terms, respectively. The KEGG pathway enrichment analysis revealed that more than 50 upregulated genes belong to metabolic pathways. More specifically, the upregulated genes were involved with the PI3K-Akt signaling pathway, the PPAR signaling pathway, insulin secretion, and glutathione metabolism (**Fig. 6A**). Most of the downregulated genes were primarily associated with the cell cycle, DNA replication, the p53 signaling pathway, and pathways related to DNA repair.

GO analysis by categorizes genes into the following 3 functional categories that were possibly associated with the up- (**Fig. 6B-D**) and down-regulated genes (**Fig. 6E-G**): biological processes (BP), cellular components (CC), and molecular functions (MF). Interestingly, multiple upregulated genes were involved in cell differentiation, positive regulation of gene expression, negative regulation of cell proliferation, regulation of transcription involved in cell fate commitment, neuronal morphology, negative regulation of cell death, and glutathione metabolic process. Moreover, the upregulation of genes associated with ion channel transport and activity, as well as synaptic function, indicates that Dex may induce the differentiation of functional neurons from CAD cells. Consistent with KEGG pathways, overall, downregulated genes were involved in the cell cycle, DNA replication, and DNA repair.

### *Validation of DEGs and expression of genes related to GR activation, neuronal markers, and catecholaminergic phenotypes*

To validate the results obtained from RNA-seq, we used qPCR to measure the expression levels of selected genes associated with observed phenotypes. We selected upregulated genes involved in cell differentiation (*CEBPB, NDRG2,* and *FGF1),* negative regulation of cell death (*IL6,* and *PPARA),* glutathione metabolism (*GSTA3),* ion channels (*SCN1A, KCNT1,* and *HCN1)* and synaptic function *(SYT2*). As shown in **Fig. 7A**, the mRNA expression levels of these genes were markedly increased in the Dex-differentiated CAD cells relative to those in undifferentiated cells. The downregulated genes that play a role in p53 signaling and the cell cycle (*GADD45b, CDK2, CCNE2,* and *E2F2*) were also selected for validation. The mRNA expression levels of these genes were also markedly reduced in the Dex-differentiated CAD cells relative to those in undifferentiated cells (**Fig. 7A**). As shown in **Fig. 7B**, the mRNA expression (fold change) of these genes in Dex-differentiated CAD cells, relative to the undifferentiated CAD cells, obtained by qPCR were positively correlated with those analyzed by the RNA-seq (Pearson r = 0.92, $R^2$ = 0.84, P<0.0001).

Besides genes analyzed from RNA sequencing, we observed a significant upregulation of *FKBP5,* a gene encoding for FK506 binding protein 51, which is a known reporter gene that indicates higher activation of

GR signaling (Bali et al. 2016; Lieberman et al. 2017; Desmet et al. 2017; Frahm et al. 2018)in Dex-differentiated CAD cells relative to those in undifferentiated cells **(Fig. 7C)**. Moreover, we observed the expression of *GAP-43*, *Tubb3*, *synaptophysin*, *Map2*, *Mapt* and *tyrosine hydroxylase,* which are the genes encoding for neuronal protein markers including GAP-43, beta3-tubulin, synaptophysin, MAP-2, Tau and tyrosine hydroxylase (TH, catecholaminergic phenotype marker) (Li et al. 2005, 2007), respectively. The expressions levels of these genes were significantly higher in Dex- differentiated CAD cells in relative to expression levels in undifferentiated CAD cells **(Fig. 7C)**. Taken together, our results suggest that Dex induces upregulation of several genes, particularly those involved with GR activation, neuronal differentiation, function, and survival. In contrast, the genes involved with cell proliferation were decreased in the presence of Dex, thereby supporting its roles in promoting neuronal differentiation.

# Discussion

Here, we proposed a novel methodology for inducing the differentiation of a catecholaminergic CNS-derived cell line, CAD cells, using the glucocorticoid receptor agonist (dexamethasone, Dex) in 1% serum-containing medium. Dex successfully transformed CAD cells from the active proliferating phase to postmitotic/neuron-like cells that entered the G0 phase and extended long neurites. The morphology and properties of the Dex-differentiated CAD cells was identical to those of the serum-free differentiated cells. However, Dex-differentiated CAD cells had the additional advantage of prolonged survival. Dex-differentiated CAD cells can be maintained in a healthy condition for at least a month, making them an effective *in vitro* model for CNS-derived catecholaminergic neurons.

It is known that in human and animals, chronic stress promotes GC release, resulting in detrimental effects, such as decrease adult neurogenesis (Pakdeepak et al. 2020) and triggering neurodegeneration (Mravec et al. 2018; Canet et al. 2018). However, various *in vivo* studies have shown that low levels of glucocorticoid can actually promote neurogenesis and neuronal survival (Glick et al. 2000; Anacker et al. 2013; Ma et al. 2018). In this study, we demonstrated an additional benefit of glucocorticoid treatment; specifically, its use as a novel method for *in vitro* neuronal differentiation.

A number of previous studies have reported that Dex treatment inhibits NPCs differentiation into neurons (Anacker et al. 2013; Kino 2015; Koutmani and Karalis 2015; Odaka et al. 2017; Nürnberg et al. 2018), in some cases, prevents maturation of differentiating neurons (Heberden et al. 2013). However, in agreement with this study, several previous studies found that Dex promoted neuronal differentiation. For example, activation of glucocorticoid receptors has been shown to induce neurite extension in differentiating neuronal stem cells (NSCs) (Androutsellis-Theotokis et al. 2013). In addition, the differentiating effects of Dex have been documented in neuroblastoma tumors (Glick et al. 2000). Moreover, the induction of cell cycle arrest and anti-proliferative effects of glucocorticoids on NPCs have been extensively reported (Sundberg 2006; Bose et al. 2010; Anacker et al. 2013). These different effects of glucocorticoid may be concentration dependent, since researchers have observed biphasic effects of glucocorticoid on NSCs self- renewal. A low concentration of cortisol enhanced proliferation of human hippocampal progenitor cells via a mineralocorticoid receptor (MR)-mediated mechanism. In contrast,

high concentrations of cortisol reduced the self-renewal of NSCs, mainly through GR(Anacker et al. 2013). In addition, cell types, brain regions, or animal sex might also be important factors, since Dex has been shown to induce differential gene expression in regions and sex-specific manners (Frahm et al. 2018).

The presence of a differentiating factor in medium with lower levels of serum is the general procedure for the induction of differentiation of several neuronal cell lines. However, serum removal alone is not enough to induce differentiation of those neuronal lines. In fact, other factors have been identified as being critical supplements for the neuronal induction. For example, retinoic acid and neuronal growth factor (NGF)must be included in low serum-supplemented media to induce the differentiation of human neuroblastoma SH-SY5Y cells and rat pheochromocytoma PC12 cells, respectively (Hu et al. 2017; Xicoy et al. 2017; Wiatrak et al. 2020). However, CAD cells are quite unique, since they can be induced to differentiate without such additional factors. However, the long-term stability and survival of the serum-free differentiated CAD cells appears to be limited. Previous reports have shown that the serum-starving cells to promote neuronal differentiation also activates apoptotic cell death (Bottenstein and Sato 1979; Howard et al. 1993; Lindenboim et al. 1995; Eves et al. 1996). This may be because of the resulting oxidative stress in serum-starved cells, which leads to massive DNA damage that can initiate apoptosis (Loi et al. 2020). In our study, we found that, consistent with previous studies, serum-free media was able to successfully induce neuronal differentiation. However, cells only survived up to 5 days in serum-free media, even when replaced with new culture medium. Perhaps it is necessary to maintain the old culture media, as it may contain protective factors for the differentiated cells (Horton et al. 2001). However, this requirement would be problematic for experiments that require media replacement routinely.

In this study, we showed that treatment with Dex in a 1% serum-supplemented media was sufficient to maintain the survival of differentiated CAD cells. These survival-promoting effects are likely due to several possibilities. Reduced serum levels in the culture media may be sufficient to minimize the level of oxidative stress-induced DNA damage and cell death. This hypothesis could be supported by some previous studies that have included low serum in differentiation protocols (Hu et al. 2017; Xicoy et al. 2017; Wiatrak et al. 2020). Another possibility is that Dex itself might act as a survival factor, thereby sustaining the differentiated cells under serum deprivation. As mentioned earlier, although glucocorticoids have been shown to be harmful to newly born neurons in some studies, they have also been reported to have neuroprotective effects through the upregulation of p21, a cell cycle regulator that also acts as the caspase-3 inhibitor (Harms et al. 2007). Lastly, the survival-promoting effects of this protocol may come from synergistic effects of Dex and 1% FBS. As shown by transcriptomic profile, several survival pathways were upregulated, whereas pathways related to apoptosis were downregulated. However, detailed mechanisms underlying these survival-enhancing effects require further investigation.

During neurogenesis, coordination of turning off the cell cycle and inducing of neuronal differentiation is tightly regulated (Ruijtenberg and van den Heuvel 2016; Urbach and Witte 2019; Marlier et al. 2020). Moreover, it may be that the inhibition of cell cycle progression is sufficient to inducing the neuronal differentiation of CAD cells. Upon serum withdrawal, the cell cycle of CAD cells is switched off, while differentiation processes are initiated (Qi et al. 1997). Additionally, a previous study showed that the

inhibition of cell cycle progression, using anti-proliferative compounds or overexpression of p53, a tumor suppressor, promoted morphological differentiation even in the presence of sufficient amounts of serum. In this study, we demonstrated that Dex, which is another potent proliferation inhibitor also exert differentiation effects in CAD cells. Hence, the differentiation of CAD cells may be the default pathway, but it is generally suppressed by proliferative pathways.

Here, we showed that more than a thousand genes were differentially expressed in Dex-differentiation CAD cells relative to the undifferentiated CAD cells. These data indicate that Dex changes the pattern of gene expression, resulting in phenotypic changes. By validating some selected genes that were associated with cell cycle arrest and cell differentiation, we showed a downregulation of genes regulating the cell cycle and p53 signaling pathway, which is known to regulate both the cell cycle and cell death (Ruijtenberg and van den Heuvel 2016; Marlier et al. 2020), consistent with previous results showing the anti-proliferative effects of Dex. In contrast, several genes involved in neuronal differentiation and negative regulators of proliferation were upregulated in Dex-differentiated CAD cells (Cortés-Canteli et al. 2002; Ménard et al. 2002; Chen et al. 2010; Lin et al. 2015; Delmas et al. 2016). Therefore, Dex might induce differentiation in CAD cells through a mechanism that coordinates cell cycle exit and the neuronal differentiation. In addition, several genes that play a role in survival pathways were also upregulated in Dex-differentiated CAD cells. Moreover, several pathways involved with DNA repair systems were downregulated, which provides evidence that DNA damage was minimized in the Dex-differentiated CAD cells. This result is consistent with our finding that Dex prolonged the cell survival after differentiation. Finally, the upregulation of genes that encode ion channels and synaptic proteins suggests that Dex may induce differentiation of cells with neuron-like physiological behaviors, as well as morphologies.

To our knowledge, this is the first time Dex has been shown to have effects on the neuronal differentiation of CAD cells. Furthermore, we show that Dex can act as a differentiating factor that causes extensive changes in CAD cell gene expression and morphology, yielding postmitotic neuronal phenotypes that resemble CNS-derived primary neurons. This method of Dex-induced CAD cell differentiation can be applied as an *in vitro* tool for studying several aspects in neurobiology including neuronal development and function.

# List Of Abbreviations

**BP** = Biological processes, **BrdU** = Bromodeoxyuridine, **BSA** = Bovine serum albumin , **CAD** = Cath.a-differentiated cells, **CC** = Cellular components, **CCNE2** = Cyclin E2, **CDK2** = Cyclin-dependent kinase 2, **CEBPB** = CCAAT / enhancer-binding protein beta, **CNS** = Central nervous system, **DAVID** = Database for Annotation, Visualization and Integrated Discovery, **DEGs** = Differentially expressed genes, **Dex** = Dexamethasone, **DMEM/F12** = Dulbecco's Modified Eagle Medium: Nutrient Mixture F-12, **DMSO** = Dimethysulfoxide, **ECACC** = European Collection of Authenticated Cell Cultures, **E2F2** = E2F transcription factor 2, **FBS** = Fetal Bovine serum, **FDR** = False discovery rate, **FGF1** = Fibroblast growth factor-1, **FKBP5** = FK506 binding protein 5, **GADD45b** = Growth arrest and DNA damage inducible beta, **GAP-43** = Growth-associated protein -43, **GAPDH** = Glyceraldehyde 3-phosphate dehydrogenase, **GO** = Gene ontology, **GR** =

Glucocorticoid receptor, **GSTA3** = Glutathione S-transferase A3, **HCN1** = Potassium/sodium hyperpolarization-activated cyclic nucleotide-gated channel 1, **IL6** = Interleukin-6, **KCNT1** = Potassium channel subfamily T, member 1, **MAP2**= Microtubule associated protein type 2, **MAPT** = Microtubule associated protein tau, **KEGG** = Kyoto Encyclopedia of Genes and Genomes, **MF** = Molecular functions, **MTT** = 3-(4,5-Dimethylthiazol-2-yl)-2,5-diphenyltetrazolium bromidefor, **NDRG2** = N-myc downstream-regulated gene 2, **NGF** = Nerve growth factor, **NPCs** = Neural progenitor cells, **PBS** = Phosphate buffer saline , **PI** = Propidium iodide, **PI3K-Akt** = Phosphatidylinositol 3 kinase- protein kinase B, **PPAR** = Peroxisome proliferator-activated receptor, **PPARA** = Peroxisome Proliferator Activated Receptor Alpha**,** **Pro** = Proliferative condition, **qPCR** = quantitative real-time polymerase chain reaction, **RRIDs** = Research resource identifiers, **RNA-seq** = RNA- sequencing, **SCN1A** = Sodium voltage-gated channel alpha subunit 1, **SDS- PAGE** = Sodium dodecyl sulfate polyacrylamide gel electrophoresis, **SF** = Serum-free differentiated condition , **SYP** = Synaptophysin, **SYT2** = Synaptotagmin 2, **TBST** = Tris buffer saline with tween 20, **TH** = Tyrosine hydroxylase, **TUBB3** = Tubulin beta 3 class lll, **$^{o}$C** = degree Celsius, **$CO_2$** = carbon dioxide, **h** = hours, **mg** = milligrams, **ml** = milliliter, **n** = Number, **pM** = picomolar, **v/v** = volume/volume, **µg** = microgram, **µL** = microliter, **µm** = micrometer, **µM** = micromolar, **%** = percentage, **i.e.** = In other words

# Declarations

**Funding:** This research project is supported by Mahidol University (NDFR20/2563), and partially by the Thailand Research Fund (IRN58W0004), and the Central Instrument Facility (CIF) grant from the Faculty of Science, Mahidol University to WS. The work was also supported by the Young Researcher Development Program from National Research Council of Thailand (NRCT), and The Science Achievement Scholarship of Thailand (SAST) to EK.

**Conflict of Interest Statement**: The authors declare no conflict of interest.

**Compliance with Ethical statement:** Not applicable

**Ethics approval:** Not applicable

**Informed consent:** Not applicable

**Availability of data and material:** All data generated or analysed during this study are included in this published article (and its supplementary information files).

**Code availability:** GEO accession numbers: GSE162087

**Author's contributions:** W.S. and E.K. designed the experiments. E.K. performed the research with the aid of K.U., N.B. and K.B. W.S. and E.K. wrote the manuscript with help from N.B. and K.B. All the authors read and approved the manuscript.

**Acknowledgements**

This research project is supported by Mahidol University (NDFR20/2563), and partially by the Thailand Research Fund (IRN58W0004), and the Central Instrument Facility (CIF) grant from the Faculty of Science, Mahidol University to WS. The work was also supported by the Young Researcher Development Program from National Research Council of Thailand (NRCT), and The Science Achievement Scholarship of Thailand (SAST) to EK.

# References

Anacker C, Cattaneo A, Luoni A, et al (2013) Glucocorticoid-Related Molecular Signaling Pathways Regulating Hippocampal Neurogenesis. Neuropsychopharmacology 38:872–883. https://doi.org/10.1038/npp.2012.253

Androutsellis-Theotokis A, Chrousos GP, McKay RD, et al (2013) Expression Profiles of the Nuclear Receptors and Their Transcriptional Coregulators During Differentiation of Neural Stem Cells. Horm Metab Res 45:159–168. https://doi.org/10.1055/s-0032-1321789

Arboleda G, Huang T-J, Waters C, et al (2007) Insulin-like growth factor-1-dependent maintenance of neuronal metabolism through the phosphatidylinositol 3-kinase–Akt pathway is inhibited by C2-ceramide in CAD cells. Eur J Neurosci 25:3030–3038. https://doi.org/10.1111/j.1460-9568.2007.05557.x

Bali U, Phillips T, Hunt H, Unitt J (2016) FKBP5 mRNA Expression Is a Biomarker for GR Antagonism. J Clin Endocrinol Metab 101:4305–4312. https://doi.org/10.1210/jc.2016-1624

Baulieu EE (1998) NEUROSTEROIDS: A NOVEL FUNCTION OF THE BRAIN. Psychoneuroendocrinology 23:963–987. https://doi.org/10.1016/S0306-4530(98)00071-7

Bilodeau ML, Ji M, Paris M, Andrisani OM (2005) Adenosine signaling promotes neuronal, catecholaminergic differentiation of primary neural crest cells and CNS-derived CAD cells. Mol Cell Neurosci 29:394–404. https://doi.org/10.1016/j.mcn.2005.03.006

Bose R, Moors M, Tofighi R, et al (2010) Glucocorticoids induce long-lasting effects in neural stem cells resulting in senescence-related alterations. Cell Death Dis 1:e92. https://doi.org/10.1038/cddis.2010.60

Bottenstein JE, Sato GH (1979) Growth of a rat neuroblastoma cell line in serum-free supplemented medium. Proc Natl Acad Sci U S A 76:514–517

Canet G, Chevallier N, Zussy C, et al (2018) Central Role of Glucocorticoid Receptors in Alzheimer's Disease and Depression. Front Neurosci 12:. https://doi.org/10.3389/fnins.2018.00739

Chen C-W, Liu C-S, Chiu I-M, et al (2010) The signals of FGFs on the neurogenesis of embryonic stem cells. J Biomed Sci 17:33. https://doi.org/10.1186/1423-0127-17-33

Chesta ME, Carbajal A, Arce CA, Bisig CG (2014) Serum-induced neurite retraction in CAD cells – involvement of an ATP-actin retractile system and the lack of microtubule-associated proteins. FEBS J

281:4767–4778. https://doi.org/10.1111/febs.12967

Cortés-Canteli M, Pignatelli M, Santos A, Perez-Castillo A (2002) CCAAT/Enhancer-binding Protein β Plays a Regulatory Role in Differentiation and Apoptosis of Neuroblastoma Cells. J Biol Chem 277:5460–5467. https://doi.org/10.1074/jbc.M108761200

Delmas E, Jah N, Pirou C, et al (2016) FGF1 C-terminal domain and phosphorylation regulate intracrine FGF1 signaling for its neurotrophic and anti-apoptotic activities. Cell Death Dis 7:e2079–e2079. https://doi.org/10.1038/cddis.2016.2

Derfoul A, Perkins GL, Hall DJ, Tuan RS (2006) Glucocorticoids Promote Chondrogenic Differentiation of Adult Human Mesenchymal Stem Cells by Enhancing Expression of Cartilage Extracellular Matrix Genes. STEM CELLS 24:1487–1495. https://doi.org/10.1634/stemcells.2005-0415

Desmet SJ, Bougarne N, Van Moortel L, et al (2017) Compound A influences gene regulation of the Dexamethasone-activated glucocorticoid receptor by alternative cofactor recruitment. Sci Rep 7:8063. https://doi.org/10.1038/s41598-017-07941-y

Eves EM, Boise LH, Thompson CB, et al (1996) Apoptosis Induced by Differentiation or Serum Deprivation in an Immortalized Central Nervous System Neuronal Cell Line. J Neurochem 67:1908–1920. https://doi.org/10.1046/j.1471-4159.1996.67051908.x

Fitzsimons CP, van Hooijdonk LWA, Schouten M, et al (2013) Knockdown of the glucocorticoid receptor alters functional integration of newborn neurons in the adult hippocampus and impairs fear-motivated behavior. Mol Psychiatry 18:993–1005. https://doi.org/10.1038/mp.2012.123

Frahm KA, Waldman JK, Luthra S, et al (2018) A comparison of the sexually dimorphic dexamethasone transcriptome in mouse cerebral cortical and hypothalamic embryonic neural stem cells. Mol Cell Endocrinol 471:42–50. https://doi.org/10.1016/j.mce.2017.05.026

Galderisi U, Jori FP, Giordano A (2003) Cell cycle regulation and neural differentiation. Oncogene 22:5208–5219. https://doi.org/10.1038/sj.onc.1206558

Ghali O, Broux O, Falgayrac G, et al (2015) Dexamethasone in osteogenic medium strongly induces adipocyte differentiation of mouse bone marrow stromal cells and increases osteoblast differentiation. BMC Cell Biol 16:9. https://doi.org/10.1186/s12860-015-0056-6

Glick RD, Medary I, Aronson DC, et al (2000) The effects of serum depletion and dexamethasone on growth and differentiation of human neuroblastoma cell lines. J Pediatr Surg 35:465–472

Götz M, Huttner WB (2005) The cell biology of neurogenesis. Nat Rev Mol Cell Biol 6:777–788. https://doi.org/10.1038/nrm1739

Hardwick LJA, Ali FR, Azzarelli R, Philpott A (2015) Cell cycle regulation of proliferation versus differentiation in the central nervous system. Cell Tissue Res 359:187–200. https://doi.org/10.1007/s00441-014-1895-8

Harms C, Albrecht K, Harms U, et al (2007) Phosphatidylinositol 3-Akt-Kinase-Dependent Phosphorylation of p21Waf1/Cip1 as a Novel Mechanism of Neuroprotection by Glucocorticoids. J Neurosci 27:4562–4571. https://doi.org/10.1523/JNEUROSCI.5110-06.2007

Heberden C, Meffray E, Goustard-Langelier B, et al (2013) Dexamethasone inhibits the maturation of newly formed neurons and glia supplemented with polyunsaturated fatty acids. J Steroid Biochem Mol Biol 138:395–402. https://doi.org/10.1016/j.jsbmb.2013.07.010

Horton CD, Qi Y, Chikaraishi D, Wang JKT (2001) Neurotrophin-3 mediates the autocrine survival of the catecholaminergic CAD CNS neuronal cell line. J Neurochem 76:201–209. https://doi.org/10.1046/j.1471-4159.2001.00017.x

Howard MK, Burke LC, Mailhos C, et al (1993) Cell Cycle Arrest of Proliferating Neuronal Cells by Serum Deprivation Can Result in Either Apoptosis or Differentiation. J Neurochem 60:1783–1791. https://doi.org/10.1111/j.1471-4159.1993.tb13404.x

Hu R, Cao Q, Sun Z, et al (2017) A novel method of neural differentiation of PC12 cells by using Opti-MEM as a basic induction medium. Int J Mol Med. https://doi.org/10.3892/ijmm.2017.3195

Kee N, Sivalingam S, Boonstra R, Wojtowicz JM (2002) The utility of Ki-67 and BrdU as proliferative markers of adult neurogenesis. J Neurosci Methods 115:97–105. https://doi.org/10.1016/S0165-0270(02)00007-9

Kino T (2015) Stress, glucocorticoid hormones, and hippocampal neural progenitor cells: implications to mood disorders. Front Physiol 6:. https://doi.org/10.3389/fphys.2015.00230

Koutmani Y, Karalis KP (2015) Neural stem cells respond to stress hormones: distinguishing beneficial from detrimental stress. Front Physiol 6:. https://doi.org/10.3389/fphys.2015.00077

Li Y, Hou LX-E, Aktiv A, Dahlström A (2005) Immunohistochemical characterisation of differentiated CAD cells: expression of peptides and chromogranins. Histochem Cell Biol 124:25. https://doi.org/10.1007/s00418-005-0017-9

Li Y, Hou LX-E, Aktiv A, Dahlström A (2007) Studies of the central nervous system-derived CAD cell line, a suitable model for intraneuronal transport studies? J Neurosci Res 85:2601–2609. https://doi.org/10.1002/jnr.21216

Lieberman R, Kranzler HR, Levine ES, Covault J (2017) Examining FKBP5 mRNA expression in human iPSC-derived neural cells. Psychiatry Res 247:172–181. https://doi.org/10.1016/j.psychres.2016.11.027

Lin K, Yin A, Yao L, Li Y (2015) N-myc downstream-regulated gene 2 in the nervous system: from expression pattern to function. Acta Biochim Biophys Sin 47:761–766. https://doi.org/10.1093/abbs/gmv082

Lindenboim L, Diamond R, Rothenberg E, Stein R (1995) Apoptosis Induced by Serum Deprivation of PC12 Cells Is Not Preceded by Growth Arrest and Can Occur at Each Phase of the Cell Cycle. Cancer Res 55:1242–1247

Loi M, Trazzi S, Fuchs C, et al (2020) Increased DNA Damage and Apoptosis in CDKL5-Deficient Neurons. Mol Neurobiol 57:2244–2262. https://doi.org/10.1007/s12035-020-01884-8

Ma XX, Liu J, Wang CM, et al (2018) Low-dose curcumin stimulates proliferation of rat embryonic neural stem cells through glucocorticoid receptor and STAT3. CNS Neurosci Ther 24:940–946. https://doi.org/10.1111/cns.12843

Marlier Q, D'aes T, Verteneuil S, et al (2020) Core cell cycle machinery is crucially involved in both life and death of post-mitotic neurons. Cell Mol Life Sci. https://doi.org/10.1007/s00018-020-03548-1

Ménard C, Hein P, Paquin A, et al (2002) An Essential Role for a MEK-C/EBP Pathway during Growth Factor-Regulated Cortical Neurogenesis. Neuron 36:597–610. https://doi.org/10.1016/S0896-6273(02)01026-7

Mravec B, Horvathova L, Padova A (2018) Brain Under Stress and Alzheimer's Disease. Cell Mol Neurobiol 38:73–84. https://doi.org/10.1007/s10571-017-0521-1

Muresan Z, Muresan V (2006) Neuritic deposits of amyloid-beta peptide in a subpopulation of central nervous system-derived neuronal cells. Mol Cell Biol 26:4982–4997. https://doi.org/10.1128/MCB.00371-06

Nürnberg E, Horschitz S, Schloss P, Meyer-Lindenberg A (2018) Basal glucocorticoid receptor activation induces proliferation and inhibits neuronal differentiation of human induced pluripotent stem cell-derived neuronal precursor cells. J Steroid Biochem Mol Biol 182:119–126. https://doi.org/10.1016/j.jsbmb.2018.04.017

Odaka H, Adachi N, Numakawa T (2017) Impact of glucocorticoid on neurogenesis. Neural Regen Res 12:1028–1035. https://doi.org/10.4103/1673-5374.211174

Pakdeepak K, Chokchaisiri R, Govitrapong P, et al (2020) 5,6,7,4'-Tetramethoxyflavanone alleviates neurodegeneration in a dexamethasone-induced neurodegenerative mouse model through promotion of neurogenesis via the Raf/ ERK1 /2 pathway. Phytother Res ptr.6983. https://doi.org/10.1002/ptr.6983

Paris M, Wang W-H, Shin M-H, et al (2006) Homeodomain Transcription Factor Phox2a, via Cyclic AMP-Mediated Activation, Induces p27Kip1 Transcription, Coordinating Neural Progenitor Cell Cycle Exit and Differentiation. Mol Cell Biol 26:8826–8839. https://doi.org/10.1128/MCB.00575-06

Pasuit JB, Li Z, Kuzhikandathil EV (2004) Multi-modal regulation of endogenous D1 dopamine receptor expression and function in the CAD catecholaminergic cell line. J Neurochem 89:1508–1519. https://doi.org/10.1111/j.1471-4159.2004.02450.x

Qi Y, Wang JKT, McMillian M, Chikaraishi DM (1997) Characterization of a CNS Cell Line, CAD, in which Morphological Differentiation Is Initiated by Serum Deprivation. J Neurosci 17:1217–1225. https://doi.org/10.1523/JNEUROSCI.17-04-01217.1997

Ruijtenberg S, van den Heuvel S (2016) Coordinating cell proliferation and differentiation: Antagonism between cell cycle regulators and cell type-specific gene expression. Cell Cycle 15:196–212. https://doi.org/10.1080/15384101.2015.1120925

Schouten M, Bielefeld P, Garcia-Corzo L, et al (2019) Circadian glucocorticoid oscillations preserve a population of adult hippocampal neural stem cells in the aging brain. Mol Psychiatry 1–24. https://doi.org/10.1038/s41380-019-0440-2

Sundberg M (2006) Glucocorticoid Hormones Decrease Proliferation of Embryonic Neural Stem Cells through Ubiquitin-Mediated Degradation of Cyclin D1. J Neurosci 26:5402–5410. https://doi.org/10.1523/JNEUROSCI.4906-05.2006

Suri C, Fung B, Tischler A, Chikaraishi D (1993) Catecholaminergic cell lines from the brain and adrenal glands of tyrosine hydroxylase-SV40 T antigen transgenic mice. J Neurosci 13:1280–1291. https://doi.org/10.1523/JNEUROSCI.13-03-01280.1993

Urbach A, Witte OW (2019) Divide or Commit – Revisiting the Role of Cell Cycle Regulators in Adult Hippocampal Neurogenesis. Front Cell Dev Biol 7:. https://doi.org/10.3389/fcell.2019.00055

Wiatrak B, Kubis-Kubiak A, Piwowar A, Barg E (2020) PC12 Cell Line: Cell Types, Coating of Culture Vessels, Differentiation and Other Culture Conditions. Cells 9:958. https://doi.org/10.3390/cells9040958

Xicoy H, Wieringa B, Martens GJM (2017) The SH-SY5Y cell line in Parkinson's disease research: a systematic review. Mol Neurodegener 12:10. https://doi.org/10.1186/s13024-017-0149-0

# Figures

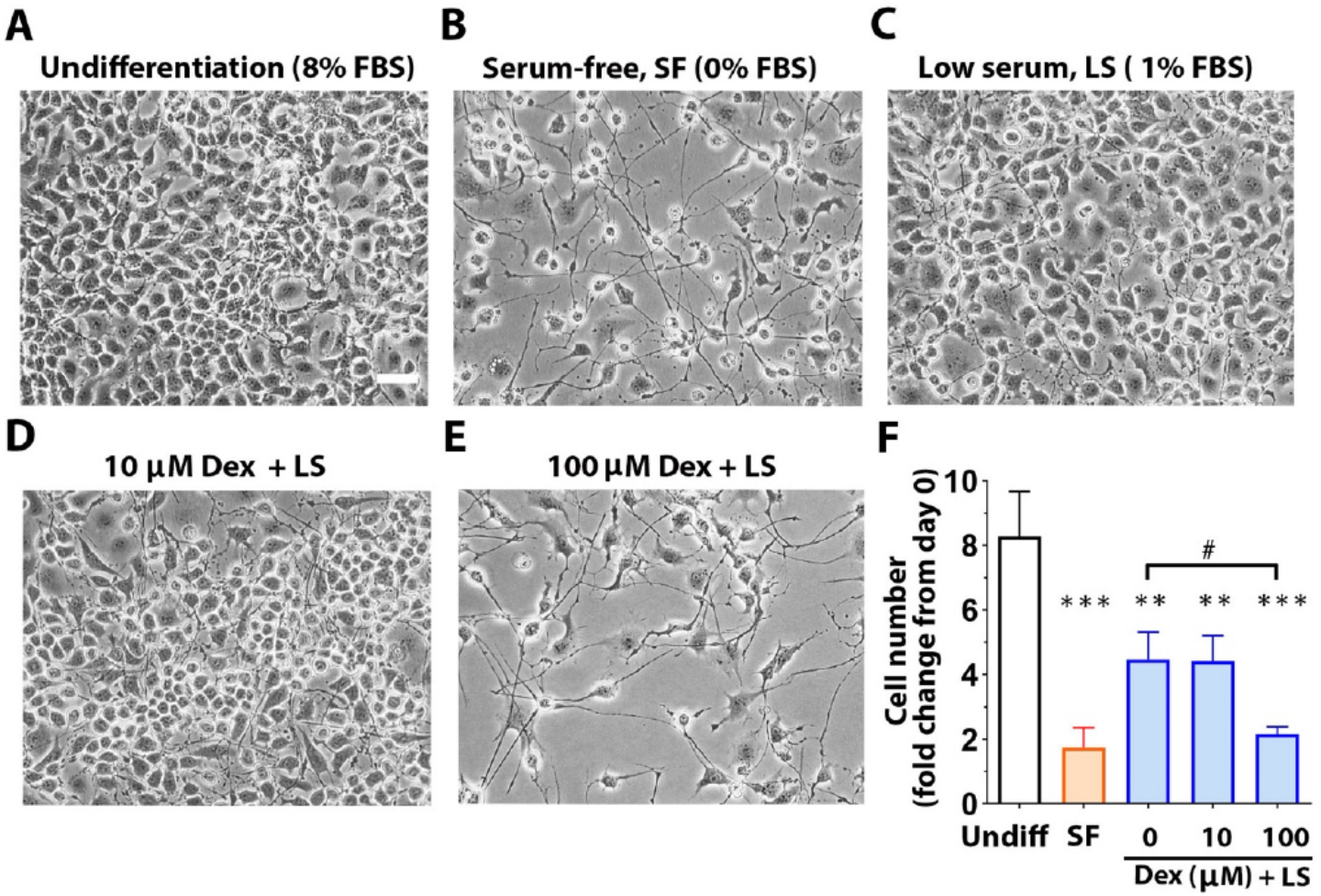


## Figure 1

Dexamethasone induced differentiation of CAD cells Representative images of CAD cells cultured in DMEM/F12 with (A) 8% FBS (undifferentiated), (B) serum-free (SF, 0% FBS), (C) Low serum (LS, 1% FBS), (D) 10 µM Dex + LS, or (E) 100 µM Dex + LS. Scale bar is 100 µm. (F) The cell number in each condition was measured by MTT assay at day 3 relative to the initial number at day 0 (n=3). ** $P < 0.01$, *** $P < 0.001$ vs. undifferentiation; # $P < 0.05$ vs. LS (One-way ANOVA with Tukey's multiple comparison test).

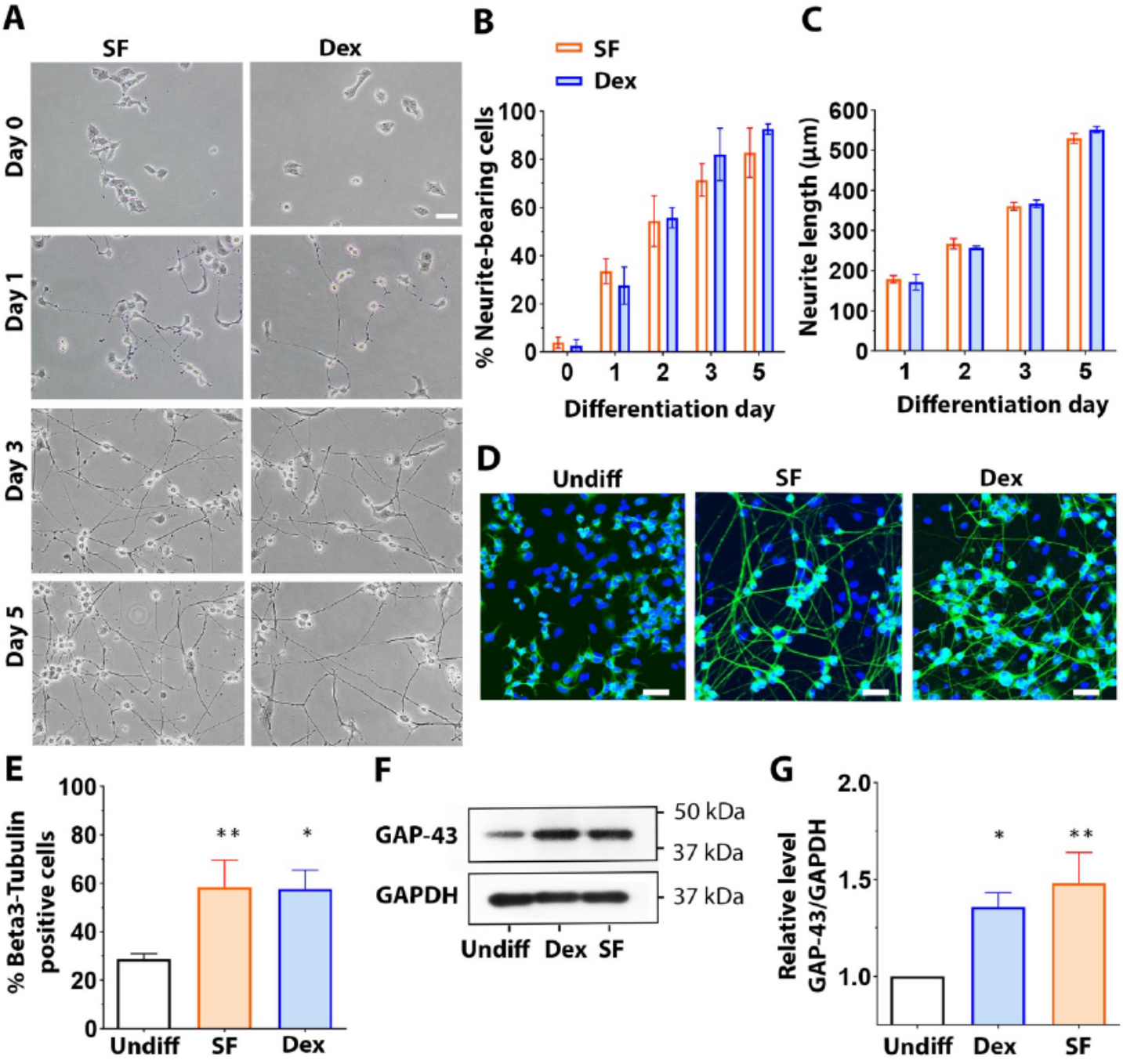


## Figure 2

Dexamethasone promoted neurite formation and elongation of CAD cells (A) Representative images showing the morphological differentiation of CAD cells differentiated by the serum-free media (SF) or dexamethasone (Dex) for 0, 1, 3 and 5 days. Scale bar is 100 μm. Quantification revealing (B) the increased number of neurite-bearing cells and (C) the length of neurites of differentiated CAD cells cultured with the differentiating media (SF or Dex) for 5 days (n=3). (D) Representative confocal images showing the expression and localization of beta-3 tubulin in undifferentiated cells (undiff) and cells differentiated by either SF or Dex for 5 days. Scale bars are 50 μm. (E) Quantification showing that beta-3

tubulin is expressed in most SF or Dex-differentiated CAD cells (n=3).(F) Western blot of growth-associated protein (GAP)-43 in undifferentiated cells and cells differentiated by SF or Dex for 5 days. GAPDH was used as a loading control. (G) Graph showing the expression of GAP-43 normalized with GAPDH (n=4). * P < 0.05, **P < 0.01 vs. undifferentiated cells (One-way ANOVA with Tukey's multiple comparison test).

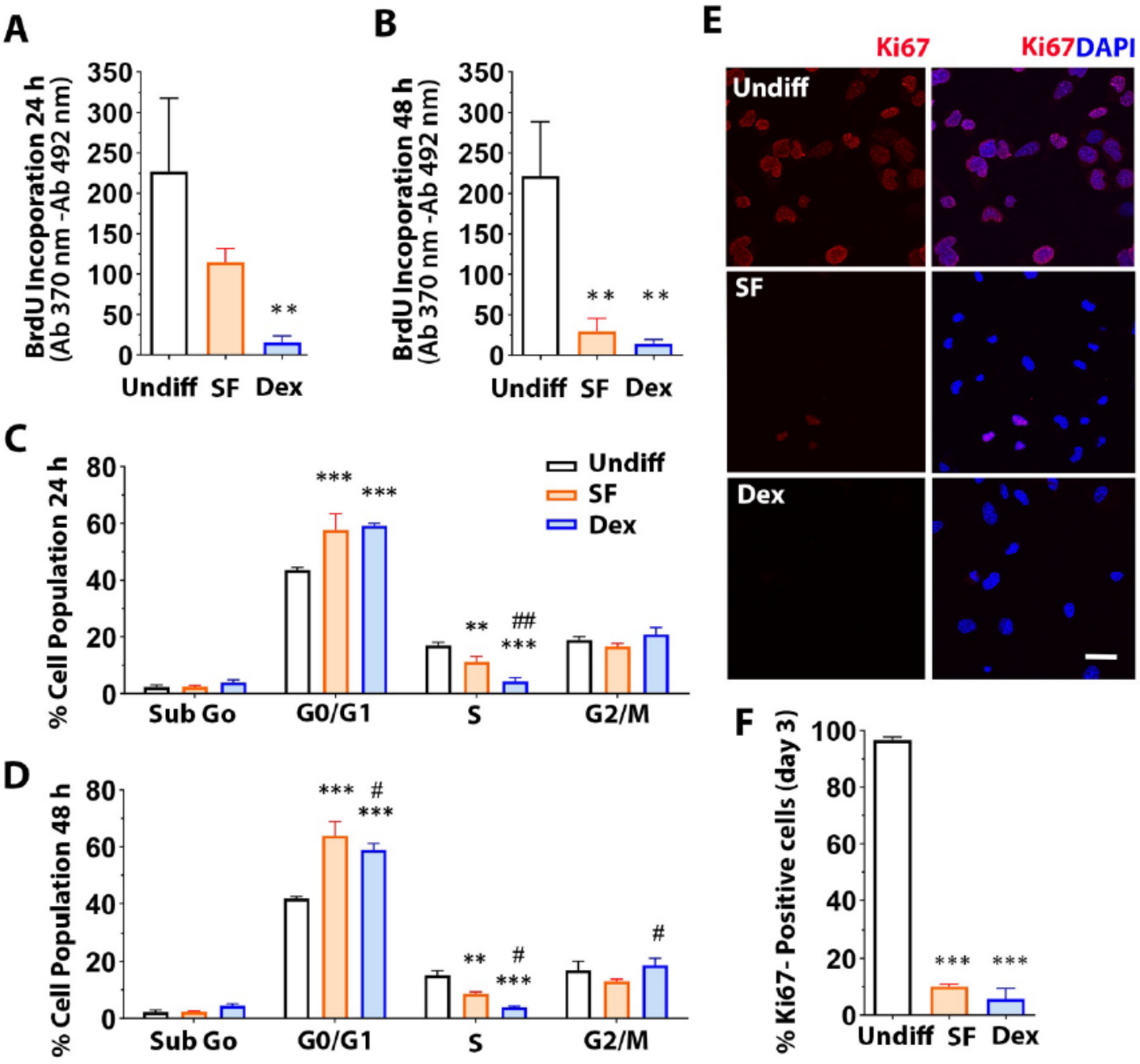


## Figure 3

Dexamethasone induced cell cycle exit and terminated proliferation of CAD cells The rate of cell proliferation as measured by BrdU assay at (A) 24 h and (B) 48 h in undifferentiated (undiff) and serum-free differentiated (SF) and Dex-differentiated (Dex) CAD cells (n=3). Flow cytometry revealing the

percentage of the cell population in each phase of cell cycle at (C) 24h and (D) 48 h in Undiff, SF, and Dex (n=3). (E) Representative confocal images showing the nuclear localization of Ki67 at day 3 in Undiff, SF, and Dex. DAPI was used to stain the nucleus. Scale bar is 30 µm. (F) Quantification showing the percentage of proliferating cells (Ki67- positive) at day 3 (n=3). **P < 0.01, and *** P < 0.001 vs. Undiff. # P < 0.05 vs. SF (One-way ANOVA with Tukey's multiple comparison test).

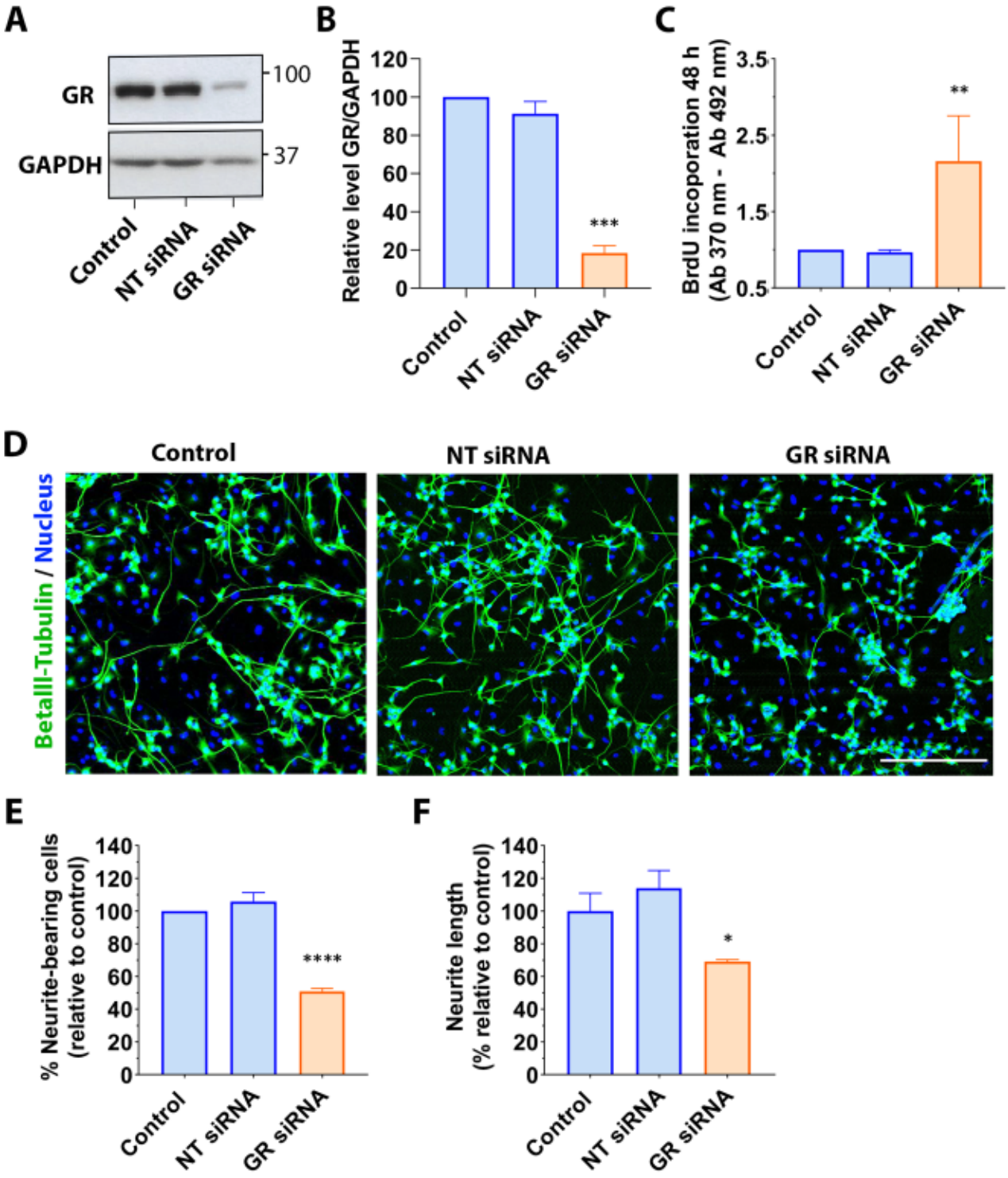


**Figure 4**

The effects of dexamethasone on CAD cells were mediated by glucocorticoid receptor (A) Western blot representing the expression of glucocorticoid receptors (GR) in undifferentiated CAD cells (Control), or the cells transfected with non-targeting siRNA (NT siRNA), or GR siRNA for 2 days. GAPDH was used as a loading control. (B) Graph showing the quantification of GR normalized to GAPDH (n=3). (C) Graph showing the rate of cell proliferation measured by BrdU assay in each indicated condition after treatment with Dex +1%FBS for 48 h (n=4). (D) Representative images showing CAD cell morphology in each condition after inducing differentiation for 72 h. Representative images showing Beta-3 tubulin and DAPI labeled neurite positive cells and nuclei, respectively. Scale bar is 300 μm. Graphs showing the quantification of (E) neurite-bearing cells and (F) neurite length in each condition after inducing differentiation for 72 h (n=3). Data were analysed from more than 800 cells for (E) and > 75 cells for (F) for each condition from at least three independent experiments. * $P<0.05$, ** $P<0.01$, *** $P<0.001$, and **** $P<0.0001$ vs Control (One-way ANOVA with Tukey's multiple comparison test).

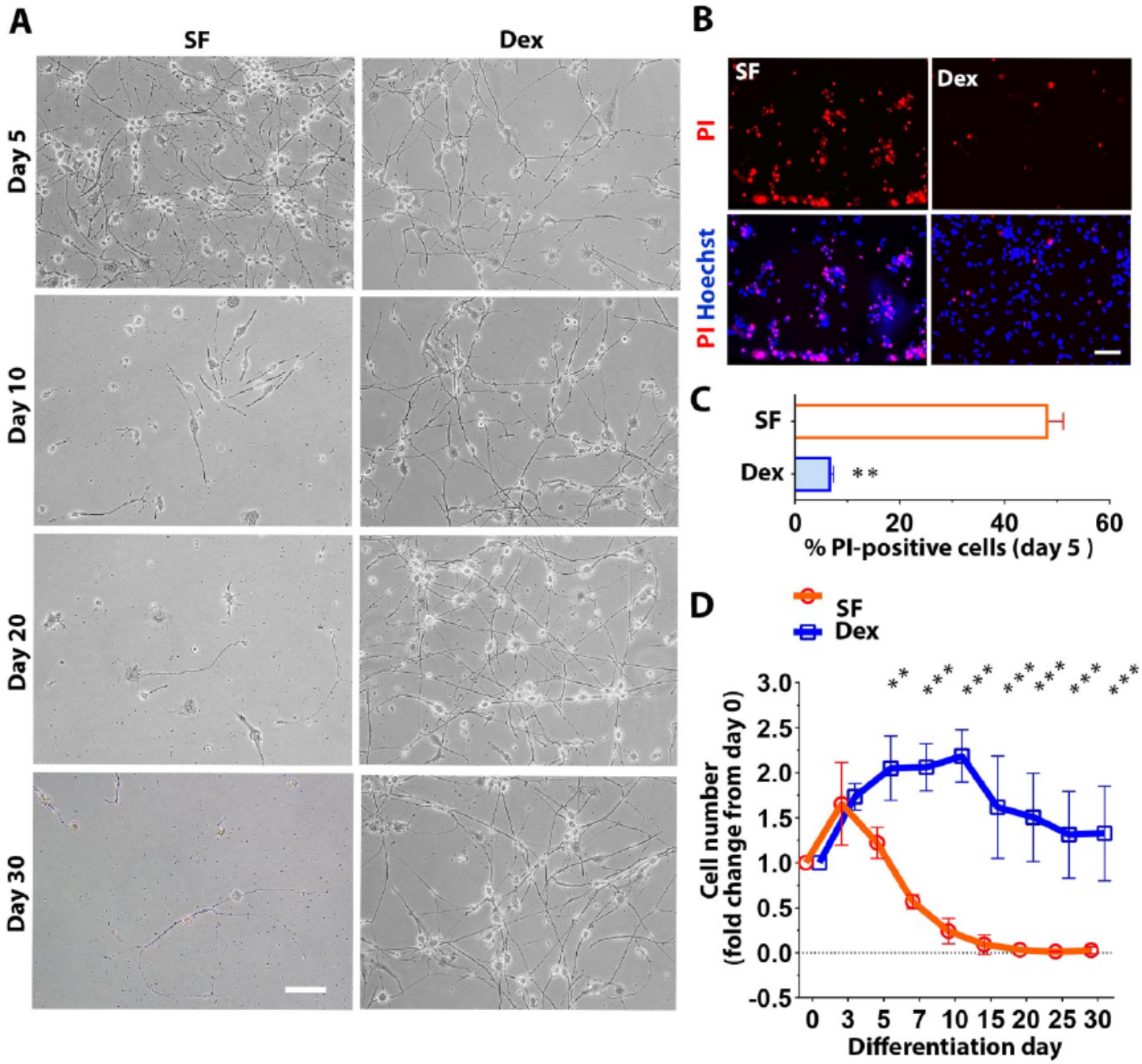


## Figure 5

Dexamethasone prolonged survival of the differentiated CAD cells (A) Representative images showing the morphological differentiation and viability of CAD cells cultured in serum-free (SF) and Dexamethasone (Dex) at day 5, 10, 20 and 30. Scale bar is 200 μm. (B) Representative images showing the presence of dead cells marked by propidium iodide (PI) in CAD cultures in SF and Dex for 5 days without replenishing medium. Hoechst indicates labeled nucleus of all cells. (C) Quantification showing the percentage of dead cells (PI-positive cells) in each condition (n=3). (D) The relative quantification of the survival number of Dex-differentiated CAD cells compared to serum-free differentiated CAD cells at

the same time point for 30 days (n=4). **P < 0.01, and *** P < 0.001 vs. SF (One-way ANOVA with Tukey's multiple comparison test).

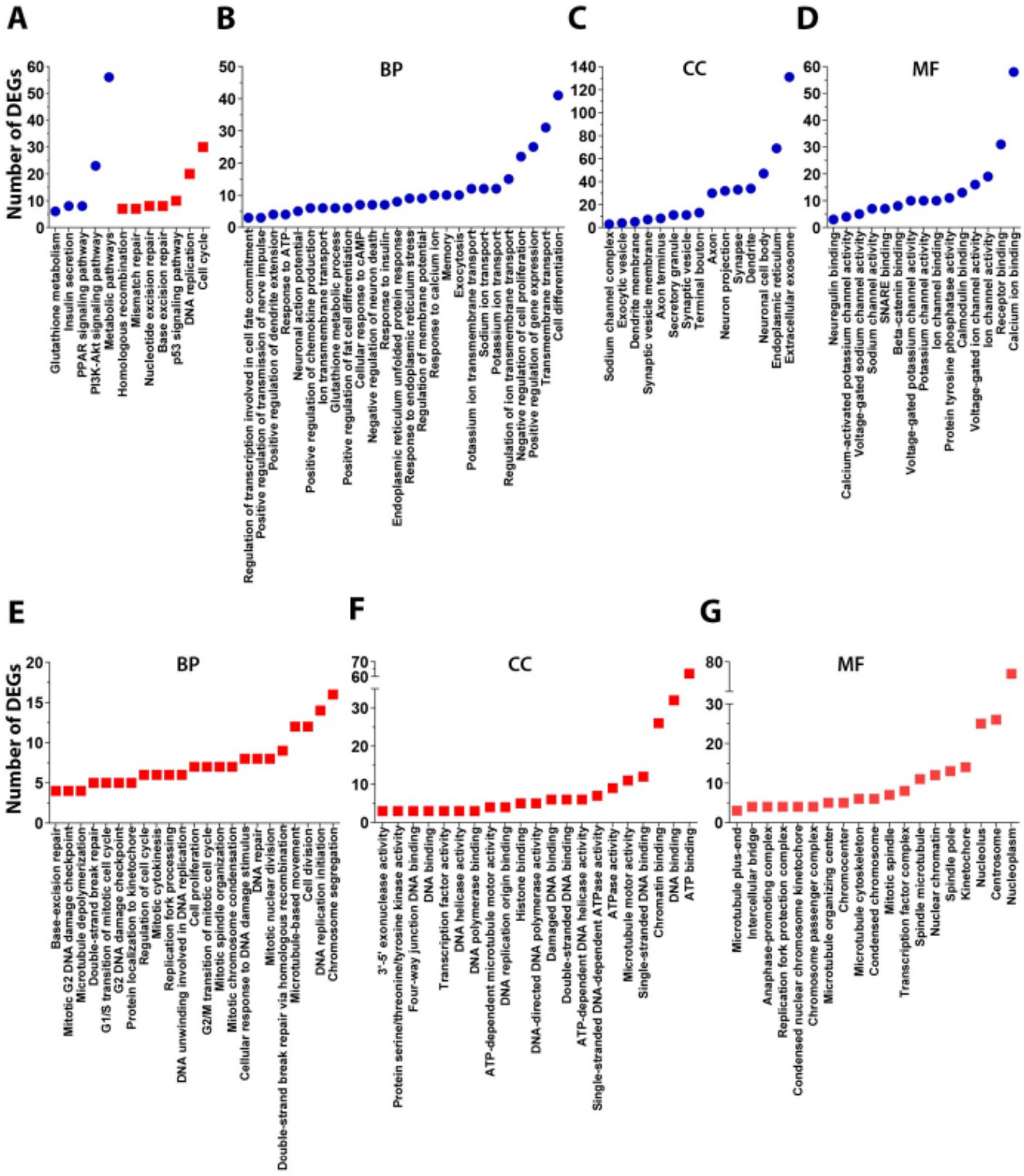


## Figure 6

Differential gene expression analysis and gene set enrichment analysis between the dexamethasone-differentiated and the undifferentiated CAD cells (A) The KEGG pathway enrichment analysis predicts the significant functional pathways with which upregulated (blue) and downregulated (red) genes were

associated (P-value < 0.05). The DEGs of each KEGG pathway are listed in Supplementary table 3-4. GO analysis classifying the significant biological processes (BP), cellular components (CC), and molecular functions (MF) of upregulated genes (B-D) and downregulated genes (E-G) in the Dex-differentiated CAD cells compared to the undifferentiated CAD cells (P-value < 0.05). The DEGs of each GO term are listed in Supplementary table 5-10.

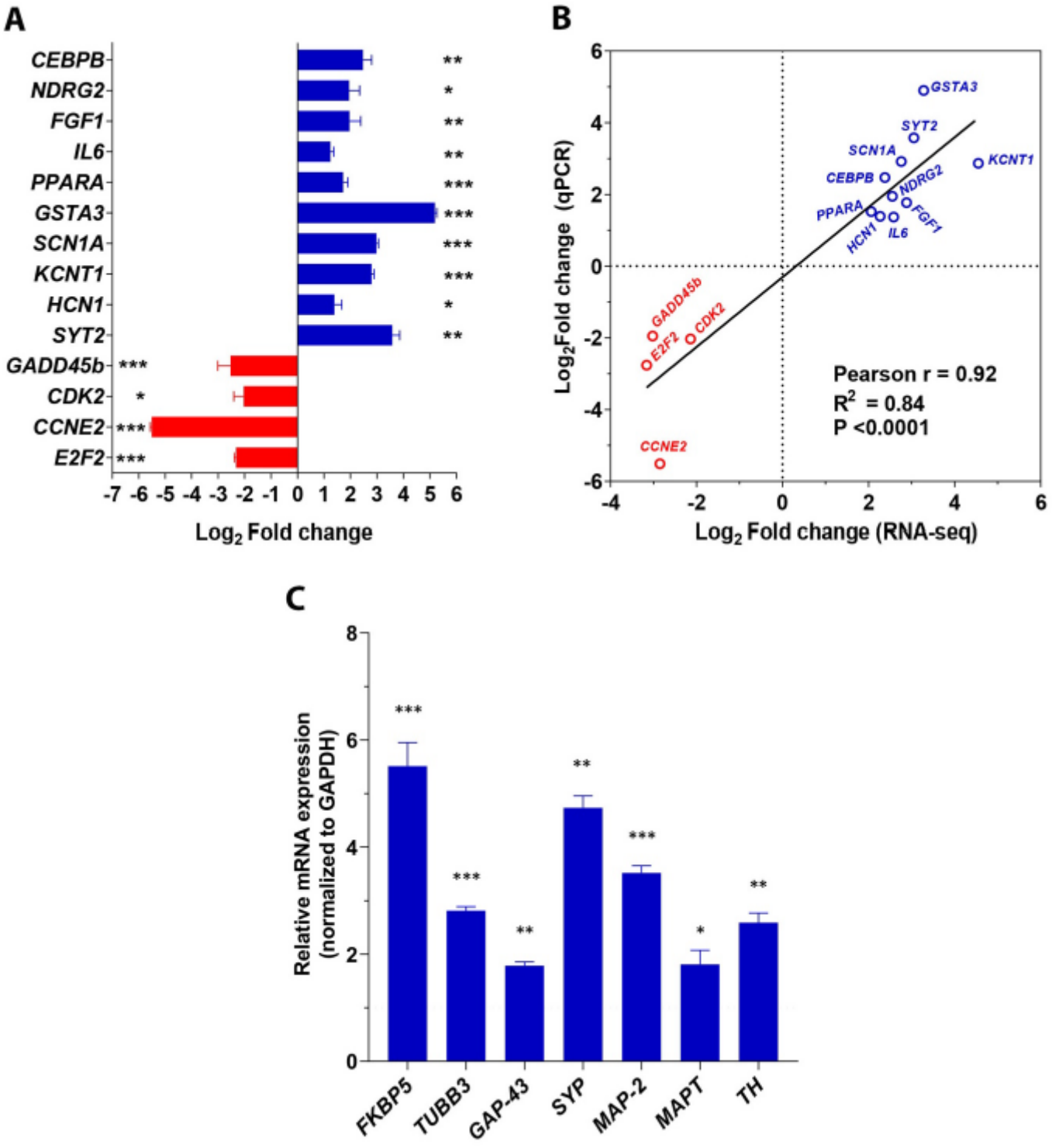


Figure 7

Validation of some upregulated and downregulated genes from RNA sequencing analysis, and genes related to GR activation and neuronal, catecholaminergic phenotypes. (A) qPCR data showing the fold change mRNA expression of selected upregulated genes involved with cell differentiation (CEBPB, NDRG2, FGF1), negative regulation of cell death (IL6, PPARA), glutathione metabolism (GSTA3), ion channels (SCN1A, KCNT1, HCN1), synaptic function (SYT2) and downregulated genes associated with p-53 signaling pathways and cell cycle (GADD45b, CDK2, CCNE2, E2F2) in Dex-differentiated CAD cells relative to undifferentiated CAD cells. The mRNA expression fold change of each validated gene was normalized to that of the GAPDH gene. (B) Pearson's correlation between mRNA fold change analyzed from RNA-seq and qPCR. Each dot represents each gene. (C) qPCR data showing the fold change mRNA expression of genes involved with GR activation (FKBP5), neuronal markers (Tubb3, GAP-43, synaptophysin, Map2, Mapt) and catecholaminergic phenotypes (tyrosine hydroxylase) in Dex-differentiated CAD cells relative to undifferentiated CAD cells from at least three independent experiments. The mRNA expression fold change of each gene was normalized to that of the GAPDH gene. * $P < 0.05$, ** $P < 0.01$, *** $P < 0.001$ vs. the undifferentiated CAD cells (Student's t-test).

## Supplementary Files

This is a list of supplementary files associated with this preprint. Click to download.

- Supplementaryexcel1.xlsx
- Supplementarymaterial.docx